energies

MDPI

*Review*

# Hydraulic Fracturing in Enhanced Geothermal Systems—Field, Tectonic and Rock Mechanics Conditions—A Review

**Rafał Moska [1,*], Krzysztof Labus [2] and Piotr Kasza [1]**

1 Oil and Gas Institute—National Research Institute, 25A Lubicz Str., 31-503 Krakow, Poland; kasza@inig.pl
2 Faculty of Mining, Safety Engineering and Industrial Automation, Silesian University of Technology, 2 Akademicka Str., 44-100 Gliwice, Poland; krzysztof.labus@polsl.pl
* Correspondence: moska@inig.pl

**Abstract:** Hydraulic fracturing (HF) is a well-known stimulation method used to increase production from conventional and unconventional hydrocarbon reservoirs. In recent years, HF has been widely used in Enhanced Geothermal Systems (EGS). HF in EGS is used to create a geothermal collector in impermeable or poor-permeable hot rocks (HDR) at a depth formation. Artificially created fracture network in the collector allows for force the flow of technological fluid in a loop between at least two wells (injector and producer). Fluid heats up in the collector, then is pumped to the surface. Thermal energy is used to drive turbines generating electricity. This paper is a compilation of selected data from 10 major world's EGS projects and provides an overview of the basic elements needed to design HF. Authors were focused on two types of data: geological, i.e., stratigraphy, lithology, target zone deposition depth and temperature; geophysical, i.e., the tectonic regime at the site, magnitudes of the principal stresses, elastic parameters of rocks and the seismic velocities. For each of the EGS areas, the scope of work related to HF processes was briefly presented. The most important HF parameters are cited, i.e., fracturing pressure, pumping rate and used fracking fluids and proppants. In a few cases, the dimensions of the modeled or created hydraulic fractures are also provided. Additionally, the current state of the conceptual work of EGS projects in Poland is also briefly presented.

**Keywords:** enhanced geothermal systems; EGS; hot dry rock; HDR; hydraulic fracturing; rock mechanics



**Citation:** Moska, R.; Labus, K.; Kasza, P. Hydraulic Fracturing in Enhanced Geothermal Systems—Field, Tectonic and Rock Mechanics Conditions—A Review. *Energies* **2021**, *14*, 5725. https://doi.org/10.3390/en14185725

Academic Editors: Dalia Štreimikienė and Tomas Baležentis

Received: 10 August 2021
Accepted: 8 September 2021
Published: 11 September 2021



## 1. Introduction

The XXI century is a time of global change in the approach in the field of energy acquisition. The current existing methods of energy production, based on conventional resources such as coal, natural gas and radioactive materials, are gradually being replaced by environmental-friendly, low-emission technologies, such as hydrogen, wind and sun farms, biomass combustion and geothermal systems. Among these modern green technologies, great potential is exhibited by so-called enhanced geothermal systems (EGS) [1]. EGS allows to extract an earth's thermal energy from impermeable (or very low permeable) hot dry rocks (HDR), which in natural conditions do not contain water, or contain a small amount [1–3]. The idea of the EGS system thermal collector is to use thermal energy of the HDR formation to heat up the process fluid in situ, extract it to the surface and use it to drive a turbine generating electricity on a commercial scale. The HDR formations are usually accessed by at least two 3–6 km deep wells, connected in a perspective layer by a network of induced fractures. The process fluid circulates in a loop between the injection and the production wells, is heated up underground in a conduction process and then releases energy at the surface (Figure 1). The main feature dividing the EGS system from the conventional geothermal system is that EGS requires creating an artificial conductivity in the reservoir, which allows gaining hydraulic connections between wells [4]. Such conductivity is obtained on EGS sites by the reservoir stimulation, which can be divided into three types, as follows: thermal, chemical and hydraulic. In thermal stimulation, cold water injection causes micro-cracking of the grains, matrix and fracture filling. Thermoelastic effects reduce the normal stress on fractures and thus promote fracture opening. The chemical stimulation consists of injecting an acid fluid to dissolve materials around the wellbore, such as cuttings from drilling and hydrothermal minerals plugging the fracture zones. For this purpose, carbonate-dissolving acids can be used. On the other hand, biodegradable chelating agents do not dissolve clay minerals and quartz. This technology was developed and used in the oil and gas industry and was adapted to deep geothermal wells to enhance the fracture network, particularly in EGS projects [5]. In hydraulic stimulation (hydraulic fracturing (HF)), an artificial fracture in the reservoir is created, or a pre-existing fracture is reopened by injecting process fluid at high pressure [6]. In the intrusive HDR strata, fresh water is most commonly used as a process fluid. In some cases, especially fracturing in tight sediments, water with some chemical additives to prevent undesirable liquid–rock interactions is also used. The polymer-based fluids, due to their increased viscosity, are characterized by better carrier properties. It allows the addition of the proppant materials, which prevent fracture closure after the operation.

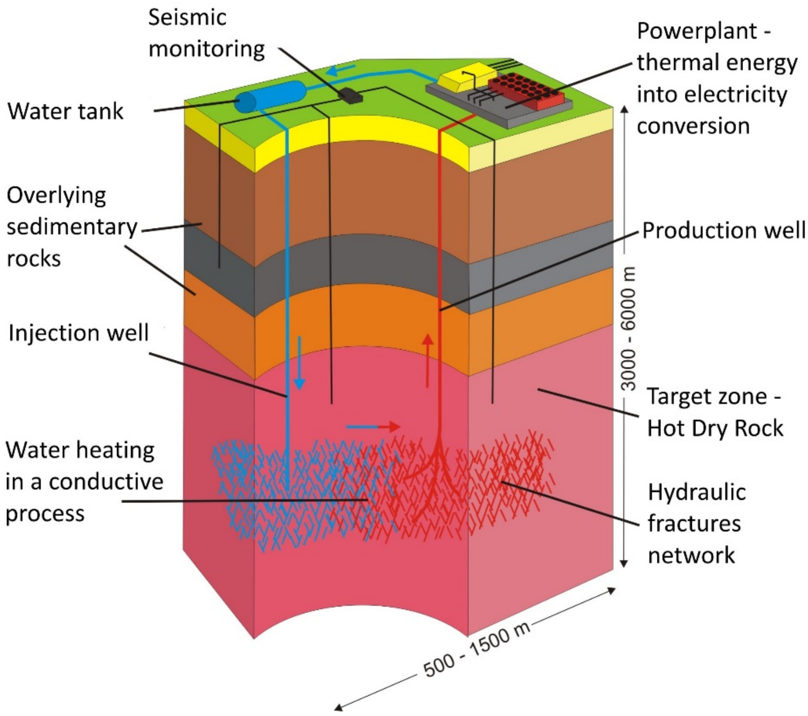


**Figure 1.** Principle of operation of a doublet enhanced geothermal system.

Designing the stimulation operations, in particular HF, requires a detailed analysis of the number of parameters such as petrophysics, petrographic and mechanic properties of the rock, as well as hydrogeologic and tectonic conditions in the field. The development of EGS technology has been ongoing since the 1970s [7]. Over the following years, a couple of research projects were carried out in order to understand the hot, deep reservoir parameters better and to improve the efficiency of heat extraction [8–10]. Some of these projects did not go beyond the research stage; however, several of them were converted into independent systems supplying energy to the power grid. With a high estimated probability, by 2050, the power of all EGS plants in the world will equal the power of hydrothermal systems and will reach the performance of about 70 GWe [1].

The aim of this paper is to collect, show and compare the major geological, tectonic and mechanical parameters of the world's EGS systems, as well as present at a glance the course and results of the hydraulic stimulation in these systems. The paper deals only with hydraulic HDR stimulation and other types of stimulation activities are not considered here. While collecting the materials, we focused on the tectonic stress regime and its influence on the fracture dimensions and propagation, as well as rock mechanic properties, such as Young's Modulus and Poisson's ratio, having a significant influence on the shape of the fracture and fracking pressure parameters.

## 2. Hydraulic Method of Stimulation Low-Permeable Reservoir

The HF operations, as one of the production stimulation methods of conventional and unconventional hydrocarbon deposits, have been known for many years (e.g., [11,12]). HF in the unconventional reservoir consists of creating or reopening the fractures in the low permeable rock and filling them with a proppant to avoid fracture closure and improve the conductivity between the reservoir and wellbore. Propagation of fracture is obtained by the hydraulic action of the fracturing fluid on the deposit. Fluid pumped from the surface through the wellbore causes stresses in the rock. If the pumping rate and pressure are large enough, inducted stresses exceed the critical stresses, which causes rock failure and fracture propagation [6,13]. Further pumping leads to fracture propagation in the vertical and horizontal directions deeper in the reservoir [14]. The fracking fluid transports the proppant grains, which fills the fractures. The process of fracturing ends when pumping with adequate capacity and pressure is stopped; after the flow stops, the fluid filtrates through the pore space of the rock, which causes a slow pressure drop. The formation stresses begin to outweigh the inducted pressure, which leads to the closure of the fracture. The proppant grains left in the fracture prevent it from fully closing and losing the hydraulic conductivity. As a result, the propped fractures constitute highly permeable arteries communicating the well and the reservoir [15]. The HDR formations are characterized by no permeability or very low permeability; therefore, reservoir stimulation, including HF, is the only method of accessing such kinds of deposits [4]. The deep wells in EGS are similar to oil and natural gas wells and in completion drilling technology. The differences concern the greater depth, a larger magnitude of stresses, higher temperatures and the presence of crystalline, igneous rocks, which are usually heat exchangers [16]. The assumptions of EGS require drilling at least two (doublets) or more (e.g., a triplet) of wells connected to each other by fracture systems in situ. The HF design process in the EGS site is similar to this kind of operation in the natural gas site. The greatest technological goal that must be met during this procedure is the prediction of the geometry of the fractures and estimation of the propagation direction between wells, so as on the one hand, gain hydraulic conductivity and on the other hand, to avoid thermal short-circuiting, leading to a decrease in temperature of the received liquid [4].

Most of the EGS fields are located in the extensional or strike-slip faulting regime; thus, in the case of vertical or subvertical wells, fractures propagate vertically with the direction more or less parallel to the wellbore. The geometry of the vertical fracture is described by basic mathematical models: KGD (Kristianowich-Zheltov, Geertsma-deKlerk) and PKN (Perkins, Kern). The models differ in the mathematical assumptions regarding the direction of deformation at the opening of the slot (vertical or horizontal). Simplifying, the models assume an elliptical fracture shape in the side view (Figure 2). The result of the model is the equation of the fracture, which binds fracture height, length, width (Figure 3) and the influence of additional parameters, such as rheology of the fracturing fluid, pumping pressure and elastic parameters of the rock [6]. Since their development, the fracture geometry models have been modified and refined many times and are offered as a key element of commercial software for oil and gas service companies.

The fracture propagation is also the subject of numerical modeling. There are three conceptual models that explain the increase in permeability during hydraulic stimulation [4,17]: (1) hydraulic fracturing (or pure opening mode)—creating new fractures in the tensile mode; (2) hydraulic jacking—reopening pre-existing fractures in tensile mode, (3): hydraulic shearing (or pure shear stimulation)—inducting slip and dilatation of natural fractures in a shear mode. Generally, hydraulic shearing is regarded as the primary mechanism of permeability enhancement in a fractured reservoir, and it is consistent with the observations of induced seismicity when the injection pressure is lower than the minimum principal stress for most EGS projects [17]. There is also a suggested mixed stimulation mechanism (MMS). The idea of MMS is that continuous pathways for flow involve both new and pre-existing fractures. The key idea is that propagating new fractures may terminate against pre-existing fractures [4].

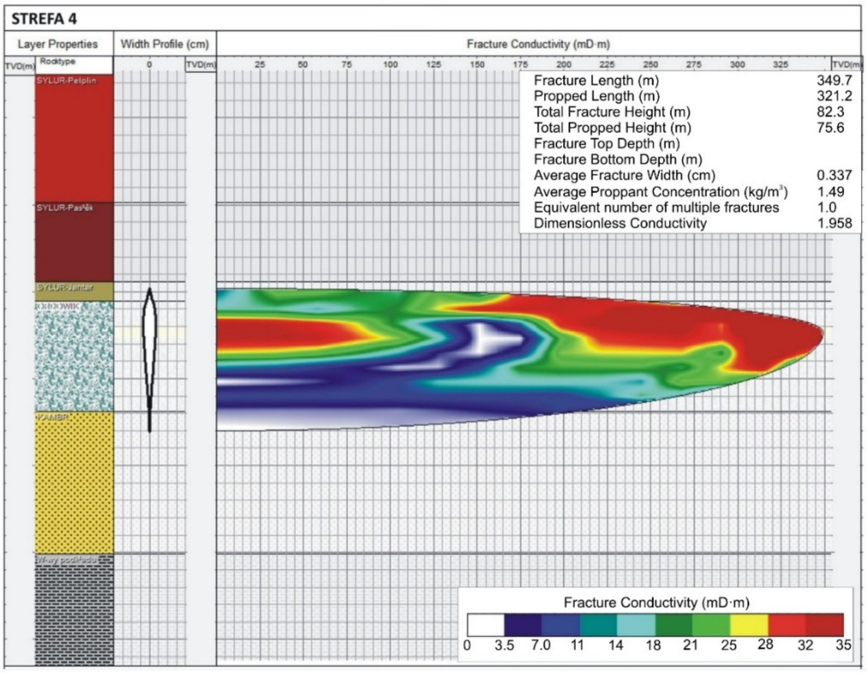


**Figure 2.** An exemplary model of a wing of the fracture. Color filling means fracture conductivity [15].

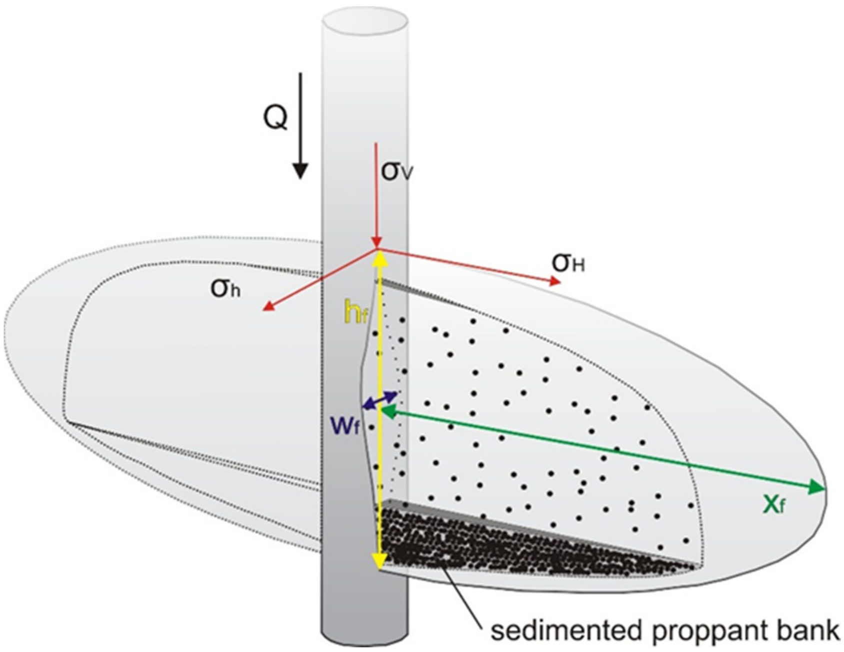


**Figure 3.** Dimensions of the fracture: $x_f$—length, $h_f$—height, $w_f$—width. Q—flow, $\sigma_V$—vertical stress, $\sigma_H$, $\sigma_h$—horizontal stresses. Based on [18].

*Rock Mechanics in the Design of Hydraulic Fracturing Operation*

Good recognition of the tectonic conditions of a field and the petrophysical parameters of productive strata, as well as top and bottom layers, is the key to design an effective HF operation in a reservoir (both geothermal and hydrocarbons). Fractures always propagate in the direction perpendicular to the minimum stress; thus, the information about the direction and magnitude of principal stresses (vertical ($\sigma_V$) and horizontal minimum and maximum ($\sigma_H$ and $\sigma_h$, respectively)) is critically important. In the normal faulting regime (extension), where vertical stress dominates ($\sigma_V > \sigma_H > \sigma_h$), vertical fractures will be created. In a strike-slip faulting regime, where the magnitude of vertical stress is less than the magnitude of one of the horizontal stresses ($\sigma_H > \sigma_V > \sigma_h$), vertical fractures propagate as well. In the reverse faulting regime (compressive), where the magnitudes of both horizontal stresses dominate ($\sigma_H > \sigma_h > \sigma_V$), a horizontal fracture propagates [19–21] (Figure 4).

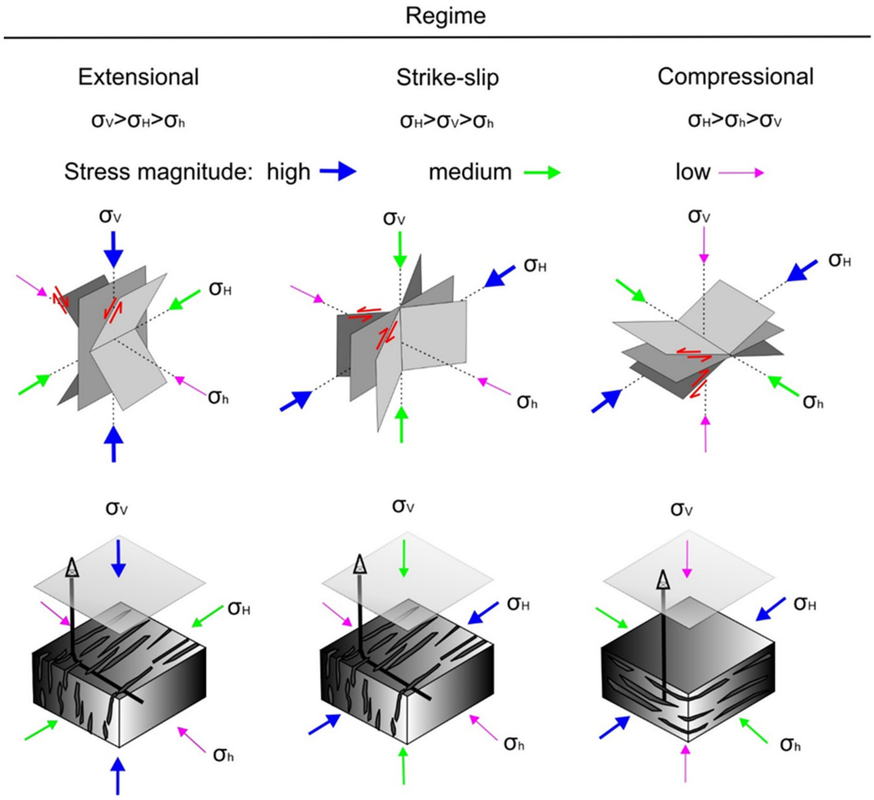


**Figure 4.** Tectonic regimes and stresses activity. Based on [20].

The stress directions in the field could be in line with the regional stress map; however, the local fluctuations of the stress state caused by local geological/tectonic conditions often occur. Directions of the $\sigma_H$ and $\sigma_h$ are determined based on focal mechanism calculation, as well as in the wells, in the way of breakout and tensile fracture analysis. The magnitude and elastic parameters of the reservoir determine the dimensions of the fracture [15]. Young's modulus (*E*) defines how much energy is required to accomplish the displacement, which is a classic linear elastic fracture mechanics concept. When increasing *E*, the height and length of the fracture increases, while width decreases. The net pressure (fracturing and closure differential pressure) also increases. Rocks with a large Young's modulus require more energy to displace. In these formations, fractures tend to be relatively narrow, and the rock is referred to as "hard" [6]. Poisson's ratio ($v$), reflecting rock deformation, occurs perpendicular to the deformation induced by the stress. In the reservoir, $v$ determines rocks' ability to fail under stress [22]. In formations of low $v$, the embedment phenomenon rises, which leads to a decrease in the conductivity of the fracture (e.g., [23–25]). Both *E* and $v$ parameters allow determining susceptibility for fracking, defined by the brittleness index [22,26–30].

## 3. Literature Review

The selected most important global EGS projects are shown in Figure 5. The authors focused on presenting the data sets and information required to design a hydraulic fracturing treatment at an EGS site, as well as the information of already performed hydraulic fracturing operations and their effects. Data include the geological information from lithology, depth of deposit, target zone temperature and method of thermal energy transport, as well as geophysical data, i.e., stress regime and magnitudes, rock mechanics parameters and ultrasonic velocities. Fracturing data include pressure, pumping rate, fracking fluids, chemical additives and proppants. Based on these data, a summary table (Table 1) was prepared. Clearly, the presented data are selective, and many elements were omitted. The described EGS projects are only part of the projects that have been conducted and implemented around the world. Projects such as Hijiori and Ogahi in Japan, Rosmanowes and Fjällbacka in Europe, Paralana in Australia and other projects in the USA are not considered in this paper. At the end of the paper, the state of current work and prospects for the EGS installation in Poland were briefly described.

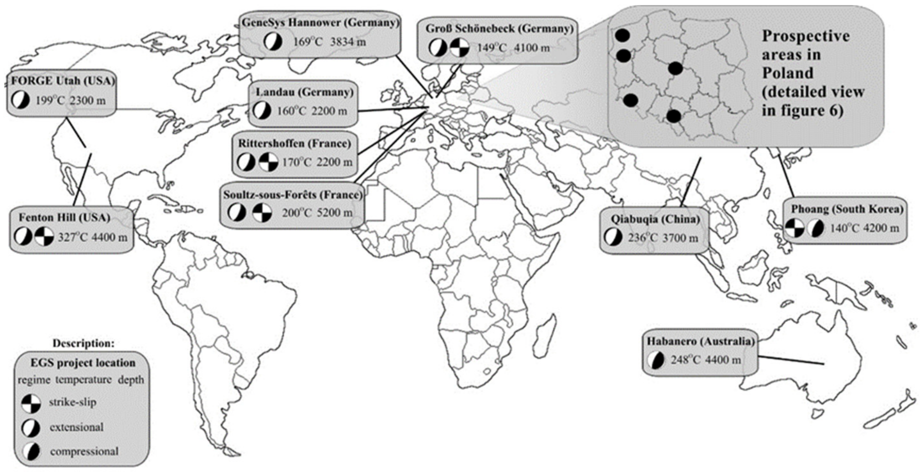


**Figure 5.** EGS projects reviewed in this paper. Beach balls represent the tectonic regime.

### *3.1. Fenton Hill (USA)*

The Fenton Hill project, located in Valles Caldera in northern New Mexico, was the world's first EGS pilot project. The aim was to develop methods of energy extracting from the granite and metamorphic HDR horizons. The target horizon consisted of biotite granodiorite and gneiss [31]. Static 3-axial tests allowed to designate the elastic parameters of the granodiorite from 4102 m depth amounted to 33 GPa and 0.12–0.22 (-) for Young's modulus and Poisson's ratio, respectively. Stress gradients of this area were estimated as $\sigma_V = \sigma_H$—25 MPa/km, $\sigma_h$—13–19 MPa/km [32].

The first phase of the project (1974–1980) involved drilling the GT-2 well to a depth of about 2930 m, where the temperature amounted to about 180 °C. The second phase, from 1979, included drilling the EE-1 production well to a depth of 3064 m and performing a fracturing treatment. Due to insufficient results, the horizontal sections GT-2A and GT-2B were drilled, where a sufficient hydraulic connection was obtained at a depth of about 2700 m. In the following years, a number of circulation tests were carried out at this site, during which a thermal power of 3–5 MWt and energy production in a binary cycle with 60 kW was achieved. In 1979, the drilling of two-directional production wells, EE-2 and EE-3, to a depth of 4390 m, where the temperature reached 327 °C. The HF treatments carried out in this well did not meet the expected results due to an unforeseen change in the stress state in the deeper parts of the stimulated horizon [16].

Re-drilling the EE-3 borehole and routing it in the area of the fractures created during the earlier HF (EE-3A) allowed for sufficient hydraulic connection. In 1986, tests of the flow in a closed loop were carried out using 37,000 $m^3$ of water, of which more than 80% was recovered. The pumping rate was between 0.64 and 1.10 $m^3$/min, whereas the wellhead pressure was between 26.9 and 30.3 MPa. The liquid temperature on the surface reached 192 °C. The formation fracturing pressure was below 19 MPa, and below this pressure, the volume of the stimulated reservoir did not increase. Long-term flow tests have been carried out since 1992, whereas water was injected at a rate of 0.75–0.90 $m^3$/min, while the temperature of the received water was over 180 °C [16].

Fenton Hill was the first site to confirm that energy production from HDR rocks on a commercial scale is possible. The experiences gained from this project were widely used in further EGS activities.

### 3.2. *Habanero (Cooper Basin, Australia)*

The Cooper Basin is located in the north-eastern part of South Australia, near the Queensland border. This area is very well recognized due to activities connected to oil and gas extraction. The crystalline basement (Big Lake Suite granite batholith) is located at a depth of 3400–3500 m (the area known as the Nappamerri Trough), where an increased geothermal gradient occurs (55–60 °C/km) [33]. Increased content of radioactive elements (e.g., uranium) causes, in this formation, local, relatively shallow zones of elevated temperature [1]. It is estimated that the batholith granites have a thickness of about 10 km. They are medium- to coarse-grained, light grey granites with aplitic and alaskite dykes and veins. Biotite is almost completely altered into chlorite, especially in shallower regions. Much of the feldspar is also altered. Their yellowish alteration is related to the oxidation process associated with the presence of permeable fractures. Granites are potassium-rich, with a silica content of 75% [33]. One of the most significant features of the Habanero area is that the stress regime of the crystalline basement is compressive (reverse faulting), i.e., the vertical stress is less than the horizontal stress. Granites remain under overpressure conditions (5000 psi above hydrostatic pressure). Among the areas of EGS projects, only Habanero and Fjällbacka (Sweden) are characterized by such kind of stress regime [4].

In 2003, the first wellbore dedicated to EGS systems—Habanero-1, with a depth of 4421 m—was drilled and completed. The investor was the private company Geodynamics Limited. The well tests have shown that the overpressure in the granite batholith is close to the fracture pressure [33]. The first hydraulic stimulation at the Habanero-1 well took place in 2003. Firstly, a series of temperature logs were recorded, the last of which showed 248.5 °C at a depth of 4390 m, with a slight upward trend in temperature over time.

In the initial stage—the fracture initiation phase, a significant part of the flow was recorded at a depth of 4254 m, whilst the lower part of the well was filled with salt to divert the flow to the above levels. After the injection of 1600 $m^3$ of water, based on the recorded microseismic events and the PTS tool, it was noted that a sufficient vertical extension of the area was achieved and that further expansion of the zone would probably occur naturally. In the main stage, water was pumped for two days at a rate of 0.79 $m^3$/min, and then the rate was increased over several days up to 1.11 and 1.43 $m^3$/min, reaching 16,350 $m^3$ total volume of water. Based on the microseismic, the SRV indicator (Stimulated Reservoir Volume) was estimated at 0.7 $km^3$, assuming the parallelogram geometry. It was a significantly higher value than the primary assumptions and higher than required for the adopted economic model of heat generation over a period of 25 years. At that time (the beginning of the 21st century), it was the largest geothermal system in HDR rocks in the world [33].

The seismic network, consisting of geophones located in eight surrounding boreholes, at depths from 100 to 850 m, up to 5 km far from the main well, was used. A total amount of approximately 11,700 events were recorded in the seismic cloud. The velocity of the P-wave in the granite at a depth below 3673 m, amounting to 5525 m/s, was recorded [33]. The elastic parameters of the granitic batholith used for modeling the breakout and tensile fractures were estimated at $E$—65 GPa, $v$—0.25 (-) [34].

The significant success of the operations conducted at the Habanero-1 well resulted in the further development of EGS projects in this area. In the following years, three more wellbores were drilled in this area: Habanero-2 (2004), 3 (2008) and 4 (2012), and two wells west of Habanero: Jolokia-1 (2010) and Savina-1 (2009) [35]. HF treatments were performed in all Habanero wells and in the Jolokia-1 well. Most treatments were performed using pure water without additives. Only in the above-described stimulation of the Habanero-1 well, NaCL-based brine was used, and in the Jolokia-1 well, high-density NaBr-based brine was used. In the years 2003–2012, 7 HFs were performed in total. From 556 to 34,023 $m^3$ of water was pumped into the reservoir, depending on the procedure. A detailed description of the performed activities was presented by Holl and Barton [35].

Barton et al. [36] presented a geomechanical model of the Big Lake Suite granite from the Habanero area. Stress magnitudes obtained from the geophysical logs and data collected during drilling clearly show the strike-slip regime in the sedimentary layers of the overlying strata, undergoing the reverse and over-thrust regime at the target zone. Therefore, at the crystalline zone, the maximum horizontal stress is the maximum principal stress. $\sigma_H$ may even amount to 150 MPa at the reservoir depth. The minimum horizontal stress $\sigma_h$ is intermediate between $\sigma_H$ and $\sigma_V$. The $\sigma_H/\sigma_h/\sigma_V$ ratio is estimated at about 1.35–1.45/1.10–1.25/1.0 at the reservoir depth. In the reverse stress regime of the Habanero region, the original N-S strike structures with a slight dip are stimulated first. Since these structures are in critical stress, stimulation occurs at pressures much less than the overburden pressure (in this case, the minimum principal stress). The fracturing process more easily induces shear in primary fault zones (sensitive to stress changes), which are optimally oriented to the stress field, than creates new hydraulic tension fractures [34–36].

Hogarth and Holl [37] formulated a few conclusions from over a dozen years of operations on wells in the Habanero EGS project. They pointed out that the fracture system in the EGS target is likely to be complex and related to brittle failure in a complex deformation history. Furthermore, the major flow path in an EGS reservoir is likely to be through pre-existing, high slip likelihood faults; thus, the in situ stress regime must be well understood so that wells can be oriented to maximize the chance of intersecting fractures with high "slip likelihood".

At the Habanero site, a 1MWe power plant was commissioned in 2013, and then by 2015, its capacity was increased to 40 MWe [1]. In the following years, the Geodynamics company closed the project due to insufficient economic viability and change in company policy [38].

### *3.3. Rhine Graben EGS Projects*

The Rhine Graben, a part of the European Cenozoic rift system, is located in Western Europe, within the borders of northern Switzeland (Basel), eastern France and southwestern Germany (Frankfurt am Main). This area is characterized by specific temperature conditions favorable for obtaining geothermal energy.

The temperature anomalies are the result of large-scale convection in the fracture system associated with nearly vertical faults crossing Cenozoic, Jurassic and Triassic sediments, as well as the Hertzian crystalline basement [39]. The tectonic regime of this area is normal to a more or less pronounced strike-slip component. Quasi-pure strike-slip events also occur, especially in the deeper part of the reservoir [40].

#### 3.3.1. Soultz-sous-Forêts (France)

The first EGS project in the Rhine Graben area was the Soultz-sous-Forêts, which was established in the 1990s, and at present includes four wells. The system is based on a triplet, consisting of one injector and two producers. The wellbores reach a crystalline basement, composed in the shallower parts of MFK porphyry granites and in the deeper parts of two-mica granite (containing biotite and muscovite) [41]. In each of the wells, there is at least one permeable naturally fractured zone in the productive horizon.

The first borehole accessing the Carboniferous granite basement at the temperature of about 160 °C at a depth of 3590 m was the GPK-1 vertical well completed in 1992. In this well, the first HF treatment in this area was conducted. In the next years (1994–2003), further wells were completed in the triplet system, which reached the granite basement at a depth of 5060–5270 m, where the temperature amounted to about 200 °C (GPK-2, 3 and 4) [39]. The distance between the wells in the productive zone is about 600 m. The directional sections of the wells are located along the N-S axis, parallel to the direction of the maximum horizontal stress [41].

The hydraulic stimulation of each of the boreholes was started by pumping tens of thousands of liters of fresh water, then brine of a density of 1.2 kg/L, in the total amount of about 800 $m^3$, initiating the fracture propagation. Then, MHF (massive hydraulic fracturing) was performed. The HF in the GPK-2 well was carried out for 6 days with a pumping rate of about 3 $m^3$/min. The wellhead and bottom pressure showed a slight but constant upward trend during pumping as a result of the shear stress-induced fracking. The maximum overpressure of 150 bar was lower than expected and indicated that the reservoir was close to the critical condition. An increase in productivity from 0.02 to 0.4 L/(s·bar) were observed [42]. In the GPK-2 and GPK-3 wells, a simultaneous stimulation was carried out to concentrate the fracturing process in the part of the reservoir between these wells. A total of 34,000 $m^3$ of water was pumped in. The wellhead and bottom pressure charts show the dependence of the pressure on the pumping efficiency, which suggested filling the pore space rather than its effective stimulation. However, the productivity factor of the GPK-3 borehole was increased from 0.2 to 0.3 L/(s·bar), while the hydraulic connection between the two boreholes was significantly improved. The GPK-4 well was of marginal production importance before stimulation. Two HFs were performed in this well. Water was pumped with a rate of 1.8–2.7 $m^3$/min, whereas a total of 9300 $m^3$ of liquid was pumped in at the first and 12,300 $m^3$ at the second frac. A high overpressure (170 bar) at the beginning of the first frac, as well as its slight decrease, may indicate an artificial fracture creation. The well productivity increased from 0.01 to 0.2 L/(s·bar); however, the hydraulic connection between GPK-3 and GPK-4 was still poor [42].

Currently, a 1.5 MW power plant is installed at the EGS Soultz site. It is planned to be developed to 3 MW [43].

#### 3.3.2. Rittershoffen (France)

The success of the Soultz project in France resulted in the commencement of another EGS in the town of Rittershoffen, about 6 km southeast of Soultz. The geological and tectonic conditions of this area do not significantly differ from Soultz; however, the 150 °C isotherm lies slightly shallower there. The tectonic regime is, like in the case of Soultz, extensional and strike-slip [44]. The project was initiated in 2004, and the first GRT-1 well was drilled after obtaining permission in 2013. The second GRT-2 (directional) well complementing the doublet system was completed in 2014 [45]. Both wells access the Rittershoffen fault zone and a crystalline target zone at a depth of about 2200 m. The temperature recorded at the bottom of the GRT-1 well (2526 m TVD) was 163 °C, while in the GRT-2 well, at a depth of TVD 2693 m, the temperature of 177 °C was measured [44]. The GRT-1 well was stimulated in three ways: thermal, chemical and hydraulic.

The hydraulic stimulation was carried out in 2013 when 3250 $m^3$ of water without proppant was pumped at a rate from 0.6 to 4.8 $m^3$/min [5]. Several hundred seismic events of the highest magnitude in the range of 1.4–1.6 were recorded [46]. The P-wave modeling of the granite target zone, based on the focal mechanisms, allowed to determine the velocity of 5600 m/s at a depth of 2550 m [47]. The magnitudes of the principal stresses, calculated based on the formulas cited from [47], for a depth of 2200 m are $\sigma_V$—54.8 MPa, $\sigma_h$—29.6 MPa, while the pore pressure is 22.5 MPa.

Since 2016, the Rittershoffen doublet EGS was integrated into the local power grid and currently generates 25 MWth of nominal thermal power [48].

#### 3.3.3. Landau (Germany)

The first German geothermal project—Landau, led by GeoX GmbH, aims to obtain geothermal energy from a fault system in the Permian sedimentary rocks and a granitic basement of the Rhine Graben. The doublet system was drilled in 2005–2006, reaching the depth of the open holes between 2100 and 2200 m and the distance between the wells of approximately 1200 m. Because of the thermal convection in the fault zone, the geothermal gradient of this area is elevated; thus, the temperature measured in the relatively shallow productive horizon amounted to about 160 °C [42].

The Gt La-1 borehole, after initial testing and cleaning, turned out to have sufficient productivity, whereas the Gt La-2 required MHF stimulation. The stimulation was carried out gradually. In the first stage, a preliminary test was performed with the wellhead pressure reaching 100 bar in peak and the pumping rate in the step-up system reaching 5.16 $m^3$/min (a total of 4600 $m^3$ of liquid). Afterward, the main HF was carried out with a wellhead pressure exceeding 110 bar and a flow rate of up to 9.0–11.4 $m^3$/min. A total of 6600 $m^3$ of liquid was pumped in [42]. In the Gt La-2 well, an acidizing treatment was also performed of 95 $m^3$ of 33% HCl, pumped at a rate of 0.6 $m^3$/min by coiled tubing, while fresh water was pumped through the annulus. The temperature logs before and after acidizing and showed that the outlet had shifted from sedimentary rocks to granite. After HF and acidizing activities, the production capacity of the Gt La-2 well increased five-fold [42]. Currently, the Landau geothermal power plant supplies 2.9 MW of electricity to the German power grid and 3MW of thermal energy [43].

#### 3.3.4. Basel (Switzerland)

Another EGS project in the Rhine Graben area was the Swiss project Deep Heat Mining in Basel. The BS-1 well in the city of Basel was completed in 2006, accessing the granite target zone. In the same year, the MHF was performed, injecting 12,000 $m^3$ of water at a wellhead pressure of 300 bar. The data analysis confirmed a consistent improvement in rock permeability of two orders of magnitude as a result of several high conductivity fracture activations. During the treatment, local seismic events of magnitude up to 2.7 were noted. A few hours later, an event of magnitude 3.4 occurred, which resulted in the wellbore pressure drop to a hydrostatic level within a few days [49]. As a result of this event, the Basel EGS project was suspended and finally terminated.

### *3.4. GeneSys Hanower (Germany)*

The GeneSys project was carried out in Hanover in 2009 and was a continuation of the GeneSys Horstberg test project. The purpose was to demonstrate the operation of the EGS installation in a single well, accessing low-permeable sedimentary formation. Two concepts of operating installation were considered. The first one assumed that cold water, pumped through the lower perforation zone, is heated up during the flow through the inducted vertical fracture and returns to the borehole in the upper perforation zone, where it is transported to the surface in the annular space. The second concept, so-called "huff-puff", was a cyclic one assumed cold water injected into a large fracture and produced back as hot water defined residence time [50,51].

The target zone was the Middle Buntsandstein sediments consisting of clay–mud–sandstone sequences, accessed by the Groß Buchholz Gt1 borehole, of 3834 m TVD. The temperature at the bottom of the well was 169 °C. From a depth of 3160 m, the well was deviated at an angle of 30°, whereas the deviation corresponded to the direction of the minimum horizontal stress. Elastic parameters of the target interval rocks varied depending on the rock type. The $E$ modulus of the sandstone ranged from 45 to 65 MPa, while $v$ ratio ranged from 0.19 to 0.22 (-). The $E$ modulus measured for clay deposits was very high for this type of rock and amounted to 49 GPa, while $v$ was 0.23 (-). For the salt layer, a limiting the horizon at the top, $E$ modulus of 33 GPa and the $v$ ratio of 0.25 (-) were assumed. $\sigma_h$ in the target interval was 72–83 MPa, which corresponded to 90% of the $\sigma_V$. The tectonic regime of this area is described as extensional; however, slight differences in the magnitude of $\sigma_V$ and $\sigma_h$ stresses indicate almost isotropic conditions. Numerical simulations of the fracture dimensions and propagation, based on the assumed pumping rate of 4.8 $m^3$/min and the total water volume of 20,000 $m^3$ of water, allowed obtaining a profile of a vertical fracture 1320 m in length, 430 m in height and 2.1 cm width [52].

The conducted minifrac tests showed a fracking pressure of 37.0 MPa when pumping with a rate of 0.1 $m^3$/min and a total liquid volume of 2.5 $m^3$. In a step-rate test, the maximum wellhead pressure of 42.0 MPa with a rate of 0.72 $m^3$/min was achieved. After the pumping, the wellhead pressure remained at a constant level, which confirms the very low permeability of the formation. The main frac was performed in 2011. Pure water without chemical additives was used. The planned 20,000 $m^3$ of water was pumped in for 5 days with a capacity of 5.4 $m^3$/min. The pumping was carried out in several stages. In each of them, the pumping rate was quickly increased to the assumed values and then held for some time at a more or less constant level, and fluctuations in pressure were observed. The wellhead pressure reached a maximum of 46.0 MPa. The observed pressure curves indicated good conductivity and negligible friction loss. Seismic monitoring did not reveal any events related to the conducted activities. Low-efficiency injection tests were conducted several months after the main frac confirmed the conductivity of the fracture system in an area of approximately 1 $km^2$. Because of the high salinity of the water, there was a salt plug trend in the wellbore; however, it was assessed as a local problem in Hanover. Finally, the GeneSys project was successful, and the experiences were used in other EGS sites [52].

### 3.5. Groß Schönebeck (Germany)

The Groß Schönebeck area is located in Germany, north of Berlin, in the north-eastern part of the North German Basin. The basin formation occurred between the Late Carboniferous and Early Permian, when the deposited volcanic rocks were covered by a Rotliegend siliciclastic sequence of alluvial fans, ephemeral streams, playa deposits and aeolian sands. Then, cyclic evaporitic sediments were deposited during the Upper Permian Zechstein. Sediments are covered by Mesozoic and Cenozoic strata [53].

Groß Schönebeck is a research area of the German Research Centre for Geosciences (GFZ Potsdam). The purpose of the GFZ EGS geothermal project was to develop technologies to increase the permeability of deep aquifers using hydraulic fracturing methods. The goal was to learn how to control the stimulation of a variety of rocks so that geothermal energy can be exploited from any kind of reservoir where it is needed [54]. The target zone consists of two types of Rotliegend deposits: low-permeable clastics at the top and volcanic (rhyolite, andesite) at the bottom [2]. These rocks, lying at a depth of 3850–4258 m, were accessed by an old hydrocarbon exploration well (GrSk 3/90), completed in 1990, and deepened in the purpose of EGS in 2000 to a depth of 4309 m [54]. In 2006, a second well (GrSk 4/05) was directionally drilled and completed in the production strata [55]. The older well was adapted as an injection well, while the other directional one as a production well. The distance between the wells at the reservoir depth was 241–470 m [56]. The temperature of 149 °C, at a depth of 4285 m and the formation pressure of about 44.9 MPa at a depth of 4220 m was recorded in the injection well [54]. Investigations of the stress state in the Rotliegend formation, based on 3D modeling and confirmed by data from HF, show the dependence of $\sigma_h \geq 0.55\ \sigma_V$ and $\sigma_H \leq 0.78$–$1.00\ \sigma_V$ in the normal to strike-slip tectonic regime. The magnitudes at a depth of about 4100 m were estimated at $\sigma_V$—100 MPa, $\sigma_h$—55 MPa and $\sigma_H$—78–100 MPa [57].

Blöcher et al. [55] compiled the parameters of the number of HF treatments performed at both wells in the Groß Schönebeck project. In 2002, in the GrSk 3/90 well, four HF treatments were performed at two depth intervals of the open hole section. HTU linear gel (cationic, hydrophilic, polymer-based) and brine were used as a fracturing fluid. Total weight of approximately 8500–8700 kg, 20/40 mesh Carbo-Lt proppant was also used in the two treatments. The pumping rate was 2.0–2.6 $m^3$/min, and the total volume of the pumped fluid was 103–129 $m^3$. The originally created vertical fractures were characterized by a half-length of 32 m, height of 72 m and width of 0.16 cm. In the same well, in 2003, two large MHF (massive hydraulic fracturing) treatments were carried out using water without proppant. One in the open hole section and the other in the slotted liner section.

About 4300 and 7300 $m^3$ of water were pumped in, with a rate of 1.44 and 2.4 $m^3$/min, respectively, which allowed to create the fracture of dimensions: 160 m half-length, 96 m height and 0.5 cm width. The GrSK 4/05 production well was stimulated three times in 2017. During the first treatment, 13,170 $m^3$ of water with 20/40 mesh quartz sand with a maximum rate of 9.0 $m^3$/min was pumped. The dimensions of the fracture were: half-length—190 m, height—135 m and width—0.8 cm. The next two HF treatments were performed using a crosslinked gel with a high-strength 20/40 mesh proppant, at intervals protected by a perforated liner; 280–310 $m^3$ of fracking fluid and 95–113 t of proppant were pumped in, with a rate of 3.0–4.0 $m^3$/min. The resulting fracture dimensions were about 60 m in half-length, 95–115 m in height and 0.53 cm in width [55].

### *3.6. Pohang (South Korea)*

The first EGS project in South Korea was the Pohang project, named after a city in the southeastern part of the Korean peninsula. The main objective of this project, which started in 2010, was to obtain a 1MW power plant in a doublet system. The drilling location was selected due to one of the highest geothermal gradients in Korea, i.e., 30 °C/km [58]. Before the EGS activities in this area, several low-temperature geothermal wells were drilled [59], as well as EXP-1 wellbore for stress field measurement in the reservoir [17]. The target zone for the Pohang EGS wells was a crystalline basement consisting mainly of Permian laminated granodiorites at a depth of approximately 2400 m to more than 4500 m. The crystalline formations are covered by andesites and crystal tuffs. These deposits are covered by the sedimentary formation of about 1 km thickness, consisting of Cretaceous mudstones and sandstones interlayered by volcanic intrusions and eruptions. The Tertiary cover is semi-consolidated siltstone of 200–400 m thick [17]. Stress models of this area, at a depth of 4.2 km, indicate two possible tectonic regimes: (1) strike-slip, where the ratio of $\sigma_H$ to $\sigma_V$ is 1.2, $\sigma_h$ to $\sigma_V$ ratio is 0.8 and the maximum horizontal stress acts in the azimuth line of 114°; the compression regime (2) (reverse faulting), where the ratio of $\sigma_H$ to $\sigma_V$ is 2.29 and the ratio of $\sigma_h$ to $\sigma_V$ is from 0.8 to 1.08–1.15 [17]. In order to obtain access to the granodiorite basement, two wells were drilled: PX-2 vertical well in 2015, of 4341 m depth, and PX-1, originally vertical, deepened directionally in 2016 to the depth of 4215 m. Both wells in the bottom sections were open holes and separated by a distance of about 600 m. The stable temperature recorded in the PX-2 well, at a depth of 4209 m (MD), amounted to 140 °C [17].

Core samples of granodiorite were collected during drilling the PX-2 well [60]. Granodiorite was consisted mainly of albite (43.1%), quartz (28.6%), microcline (13.7%) and muscovite (10.1%) and was characterized by a volumetric density of 2.63 g/$cm^3$ and a porosity of 0.48%. The performed uniaxial compressive strength tests allowed estimation of the average UCS at 106.7 MPa, and the average $E$ modulus and $v$ ratio of 33.5 GPa and 0.21, respectively. Triaxial tests were also performed in several steps of confining pressure. The average measured cohesion factor was 15.2 MPa, whereas the angle of internal friction was 60.2°. The average measured velocities of the ultrasonic P- and S-waves amounted to 4336 and 2676 m/s, respectively, which resulted in the dynamic $Ed$ modulus of 44.9 GPa [60]. However, these tests were not being performed at the reservoir conditions. Ultrasonic velocities measured during acoustics in this interval were 5920 and 3290 m/s, respectively, for the P- and S-waves, which means that the values measured in situ are higher by 36.4 and 22.7%, respectively. The observed increases are consistent with the literature data cited by Kwon et al. [60]. For Troy granite, increases of 40% and 20% for P- and S-wave, respectively, occurred, while the pressure was increased from atmospheric to 40 MPa. These value compilations allow easy assessment of how much the mapping of reservoir conditions during laboratory tests has an influence on the wave velocities.

Several HF activities were performed on the Pohang site [58]. The first treatment occurred in 2016 in the PX-2 well, where 1970 $m^3$ of water was pumped. The maximum wellhead pressure was 89.2 MPa, while the maximum pumping capacity reached 2.8 $m^3$/min. The stimulation mechanism was interpreted as a combination of tensile fracture extension and hydraulic jacking. The second HF was performed in 2016 in the PX-1 well, where 3907 $m^3$ of water was pumped in a period of 14 days, with a maximum reservoir pressure of 27.7 MPa and a pumping rate of 1.1 $m^3/min$. As a result of the conducted work, the transmissivity of the rock surrounding the PX-1 well increased approximately 6.4 times. The stimulation mechanism was interpreted as hydraulic shearing with hydraulic jacking. The seismic monitoring recorded the maximum magnitude of the events of 1.7 and 2.2, after the shut-in stage, in the PX-2 and PX-1 wells, respectively. A good correlation between the amount of the injected liquid and the magnitude of the seismic event in both wells was observed. The observed seismic maxima occurred during periods of the large total volume of liquid injection [17]. In 2017, the second HF on the PX-2 well was carried out at a wellhead pressure of 90 MPa, during which the maximum magnitude of the recorded seismic events amounted to 3.1. Another treatment in the PX-1 well was performed in the same year in the form of a Cyclic Soft Stimulation (CSS), consisting of pumping the liquid alternately with low and high rates to reduce the risk of induced seismicity. Recorded seismic events during these works did not exceed a magnitude of 2.0 [61].

On 15 November 2017, an earthquake of a relatively large magnitude of 5.5 occurred in the Pohang area, which resulted in the discontinuation of the EGS Pohang program. Ellsworth et al. [62], based on modeling the pore pressure variability in rocks, suggest that the increase in the pressure may initiate local seismic events in fault zones, which may accumulate into larger seismic events. A number of aftershocks were recorded, while the largest one was on 11 February 2018 (4.8) [63].

### 3.7. FORGE Utah (USA)

The EGS project, led by the U.S. Department of Energy's Frontier Observatory for Geothermal Energy (FORGE), is located about 300 km southwest of Salt Lake City, Utah. In earlier years in this area, conventional geothermal energy was obtained (Blundell Thermal Power Station, UT, USA). The aim of the project, established in 2016, was to demonstrate that the EGS installation can be commercially used for large-scale energy production. The geothermal collectors of this area are Tertiary plutonic Mineral Mountain rocks, consisting of diorite, granodiorite, quartz monzonite, syenite and granite. The main minerals are plagioclase, K-feldspar and quartz, with a low content of biotite, hornblende and clay minerals [64]. The stress regime of this area is normal [65].

In 2017, a vertical borehole was completed (58–32), reaching 2290 m deep, where the temperature of 199 °C was recorded. In the interval of the crystalline rocks (1329 m in total), granite and quartz monzonite with low permeability mostly occurred. Microscanner images and televiewer logs confirmed that the $\sigma_H$ in this wellbore tends NNE-SSW. The $\sigma_h$ gradient is defined as 16.7–17.6 kPa/m and allows calculation of the magnitude of about 38–40 MPa in the productive interval. In the case of the $\sigma_V$, the gradient is defined as 25.6 kPa/m, which determines the magnitude of about 59 MPa at a depth of 2300 m [65]. In 2017 (directly after completion) and in 2019, an open hole interval was stimulated. Minifrac tests, DFIT, and step rate tests were carried out with a pumping rate of 1.43 $m^3/min$ and pressure of about 27.6 MPa. Calcium carbonate (200 mesh) was also pumped to slightly prop the fractures taking fluid and enhancing the differentiation between fractures identified in pre- and post-FMI logs.

In 2019, a number of HFs were carried out in the open-hole part at the bottom of the well and in the two above perforated intervals. Tests were designed to determine the viability of stimulating fractures with different orientations behind the casing. The lower perforated zone was located in the region of critically stressed fractures, trending NNE parallel to $\sigma_H$, which means that these fractures would be the easiest to shear, dilate and propagate. The uppermost zone contained fractures oriented at a high angle to $\sigma_H$ (noncritically stressed). This zone was represented with the upper limits of the pressures required to stimulate the granitoid [65,66]. In the open hole section, the results were similar but slightly lower than those of the 2017 tests, suggesting the fracture system had developed some degree of permanence. The formation readily took fluid at modest injection rates of 2.38 $m^3$/min, which allows concluding that the hydraulic connection between the 58–32 well and the planned boreholes will be possible. The lower perforated zone was also successfully treaded. The fracturing pressure in the critically stressed area was 29 MPa, with a pumping rate of 0.8 $m^3$/min. The shallow, noncritically stressed zone was treated at the pressure of 45 MPa. During the treatments, a number of fracture closure pressure interpretations using various methods were also conducted.

The closure pressure increased with the pumping rate and the volume of the pumped water, which indicates the poroelastic effect and the presence of pre-existing natural fractures [66].

Project FORGE Utah is currently underway. Drilling a production borehole, accessed to the fracture network created in well 58–32 is planned, then loop test and build a power plant [67].

### 3.8. Qiabuqia (China)

The Qiabuqia geothermal site is located in the north-eastern part of the Qinghai–Tibetan Plateau. In the geological past, this area was uplifted several times, and igneous intrusion caused a local thermal anomaly to spread along the deep fault zones. The target HDR zone, below 3000 m, is built mainly from the Mid-Late Triassic Indonesian granite characterized by low porosity (2–5%) and very low permeability (0.2–0.7 mD). The overlying rocks are Neogene mudstones and Quaternary sandstones [68]. The Qinghai–Tibetan Plateau is under the tectonic influence of the Indian Ocean Plate and the Eurasian Plate. The focal mechanisms recorded in this area indicate that $\sigma_H$ in an NE 50–60° direction dominates (which is approximate to the direction of plate extrusion), whereas $\sigma_h$ is in an NW direction consistent with the expansion of the Gonghe basin. The stress regime in this area is strike-slip, turning into compressional in the southern part. The magnitude of $\sigma_V$ is based on computer modeling at 95–100 MPa and $\sigma_H$ at 85–92 MPa, while the magnitude of $\sigma_h$ at 68–72 MPa, at a depth of about 3700 m, was estimated [69]. The elastic parameters of the Qiabuqia granite were estimated as *E*—40–56 GPa and *v*—0.25–0.33 (-) [68].

The EGS project currently underway in this area involves a triplet system, including one injector and two producers. The target zone is drilled through four wells: GR1, GR2, DR3 and DR4. At the bottom of the deepest one (GR1, completed in 2017), a temperature of 236 °C at a depth of 3705 m was recorded.

The numerical simulations of fracturing operations in the GR1 well have been performed so far. Above the described stress magnitude, the mechanical properties of the rock as well as using of 50# crosslinked gel with HSP 20/40 mesh proppant were assumed. By increasing the fracture length, the width and fracture extension were observed during the increase in the pumping rate. The length of the fracture wing reached 600 m, whereas the height of about 100 m. The width, assuming the pumping rate of 6 $m^3$/min, exceeded 5 mm. An increase in the length of the wing and height was noted during pumping of up to 12,000 $m^3$ of fluid. Continuation pumping resulted in a further increase in the length, but at the same time, a significant decrease in the height. The highest proppant concentration and conductivity was achieved at the bottom of the fracture.

About 100 m in length of the fracture wing, at the farthest distance from the wellbore, has not been propped [68].

The modeling indicated that the tensile strength of the rock, as well as Young's modulus, had a significant effect on the fracture geometry, while porosity, permeability and Poisson's ratio had little effect. In the case of the slickwater-based stimulation scenario, low pumping rates of 0.5–3 $m^3$/min were proposed to avoid the use of high-power fracturing equipment, and total liquid volumes of 12,000 to 20,000 $m^3$ of slick to obtain the desired fracture network [69].

Based on the numerical simulations, a triplet system located at the line of the maximum horizontal stress (NE-SW) azimuth and separated from each other by about 300–500 m was designed. Forecasts of the thermal and energy efficiency for this system were also prepared [69].

**Table 1.** Selected geological, tectonic and fracturing data compilation from EGS sites.

| EGS Site, Activities Duration | Productive Layer Depth (m) | Temp. (°C) | Lithology, Stratigraphy | Stress Regime | Stress Magnitudes: $\sigma_V$, $\sigma_H$, $\sigma_h$ (MPa), Pore Pressure: $P_p$ (MPa) | Ultrasonic Velocities $V_P$, $V_S$ (Compressional, Shear Wave) (m/s), Elastic Parameters: Young's Modulus *E* (GPa), Poisson's Ratio *v* (-) | Fracturing Fluid | Estimated Fracture Dimensions: l—Half Length (m), h—Height (m), w—Width (mm) |
|---|---|---|---|---|---|---|---|---|
| Fenton Hill (USA) 1974–1995 | About 4400 [EE-2 well] [16] | 327 at 4390 m [16] | Core samples from EE-2 well: granodiorite, gneiss [31] | Strike-slip/normal [32] | Estimated gradients: $\sigma_V$ = $\sigma_H$—25 MPa/km, $\sigma_h$—13–19 MPa/km, $P_P$—10 MPa/km [32] | 3-axial lab test, confining: 20 MPa EE-2 core, 3916 m depth: *E*—15–22, *v*—0.12–0.17. 4102 m depth: *E*—33, *v*—0.12–0.22 [31] | MHF—fresh water [32] | |
| Habanero Cooper Basin (Australia) 2003–2016 | About 4400 [33] | 248.5 [33] | Syenogranite, medium and coarse-grained [34] | Strike-slip (overlay); reverse, over-thrust (batholith target zone) [35] | At 4267 m $\sigma_V$—97.9 $\sigma_H$—150.9 $\sigma_h$—124.4 $P_P$—73.1 [35] | From modeling at 3657 m TVD: *E*—65, *v*—0.25 [36]. From logging at 3674 m (granite) $V_P$—5525 [44] | Mostly fresh water [33], water, NaCl- and NaBr-based brine [34] | |
| Rhine Graben EGS projects (Western Europe): Soultz-sous-Forêts, 90-present Landau, 2005/6-present Rittershoffen, 2013-present | Soultz 5200 [39] Landau 2200 [42] Ritters. 2200 [44] | Soultz about 200 [39] Landau about 160 [42] Ritters. about 170 [44] | Porphyric granites MFK, two-mica granites. Carboniferous [41] | Mixed, normal and strike-slip [44] | At 2200 m: $\sigma_V$—54.8 $\sigma_V$> or <$\sigma_H$ $\sigma_h$—29.6 $P_P$—22.5; calculated, based on equations from [47] | Estimated *E* for pure granite at the target zone—up to 80 GPa, at the zones of increased hydraulic conductivity, and clay content may be significantly lower. [70] | Soultz—frac initiation: brine, then MHF—fresh water [42] Rittershoffen—MHF: water without proppant [5] | |
| GeneSys Hannower (Germany) 2005–2013 | 3834 [52] | 169 [52] | Low permeable Buntsandstein sediments, Permian [50,52] | Normal [52] | $\sigma_h$—72–83, $\sigma_h$ = 0.9 $S_V$ [52] | From lab tests and log, sandstones: *E*—45–65, *v*—0.19–0.22; clays: *E*—49, *v*—0.23 [52] | Fresh water [52] | l—1320 h—430 w—21 [52] |
| Groß Schönebeck (Germany), 2006-present | About 4100 [57] | 149 at 4285 m [54] | Clastic and volcanic rock (rhyolite, andesite) Rotliegend, Permian [2] | Normal—strike-slip $\sigma_h \geq 0.55\ \sigma_V$, $\sigma_H \leq$ 0.78–1.00 $\sigma_V$ [57]] | $\sigma_V$—100, $\sigma_H$—78–100, $\sigma_h$—55 [57] $P_P$—44.9 at 4220 m [54] | Volcanic rocks: *E*—55 *v*—0.20 Sediments: *E*—55 *v*—0.18 [20] | HTU linear gel, brine, Carbo-Lt 20/40; MHF—fresh water or with quartz sand 20/40 mesh, crosslinked gel with high strength 20/40 mesh [55] | l—32 h—72 w—1.6; MHF: l—160, h—96, w—5 [55] |

**Table 1.** *Cont.*

| EGS Site, Activities Duration | Productive Layer Depth (m) | Temp. (°C) | Lithology, Stratigraphy | Stress Regime | Stress Magnitudes: $\sigma_V$, $\sigma_H$, $\sigma_h$ (MPa), Pore Pressure: $P_p$ (MPa) | Ultrasonic Velocities $V_P$, $V_S$ (Compressional, Shear Wave) (m/s), Elastic Parameters: Young's Modulus $E$ (GPa), Poisson's Ratio $v$ (-) | Fracturing Fluid | Estimated Fracture Dimensions: l—Half Length (m), h—Height (m), w—Width (mm) |
|---|---|---|---|---|---|---|---|---|
| Pohang (South Korea) 2010–2017 | About 4200 [17] | 140 at 4209 m [17] | Laminated Granodiorite, Permian [17] | Strike-slip /reverse [58] Strike-slip [71] | $\sigma_V$—107, $\sigma_H$—133–153, $\sigma_h$—98–119 [58] $\sigma_V$—110, $\sigma_H$—115–138, $\sigma_h$—81–105 [71] | $V_P$—4336, $V_S$—2676 $E_d$—44.9 (laboratory tests, atmospheric conditions); $V_P$—5920, $V_S$—3290 (sonic logging) [60] | Fresh water [17] | |
| FORGE Utah (USA) 2016-present | about 2300 [65] | 199 [65] | Tertiary granites, quartz monzonites, monzonites [65,66] | Normal [65] | Based on gradients [65], at a depth of 2290 m: $\sigma_h$—38–40, $\sigma_V$ -59. | Granite sample from 52–21 well, 3-axial test, confining pressure 55 MPa: $E$ -73.7, $v$—0.22. [72] | | |
| Qiabuqia (China) 2016/17-present | about 3700 [68] | 236 [68,73] | Middle triassic granite, Anisian [73] | Normal [69] | Based on modeling at 3700 m $\sigma_V$—95–100 $\sigma_H$—85–92, $\sigma_h$—68–72 [69] | $E$—40–56 $v$—0.25–0.33 [68] $E$—42 $v$—0.23 [69] | For modeling was assumed: #50 crosslinked gel with HSP 20/40 proppant [68] | l—up to 600 h—about 100 w—5 [68] |
| Poland (prospective EGS areas): Karkonosze Mountains, Gorzów Block, Mogilno-Łódź Trough, Szczecin Trough Upper Silesian Block | about 4000 about 4300 about 5700 [2] about 5000 [74] about 5000 [74] | 165 153 175 [2] above 150 [74] 170 [74] | Upper Carboniferous granire, Lower Permian volcanic rocks Low-permeable Triassic sediments [2] Permian or Carboniferous sediments [74] Carboniferous sediments [74] | Western Poland—normal with strike-slip component [75,76] Upper Silesian Block—strike-slip [77] | $\sigma_V$: Karkonosze Mount.—96; Gorzów Block—103; Mogilno-Łódź Trough—120–153; Szczecin Trough—120; Upper Silesian Block—120. Based on assumed average rock density from [78] | | Fracturing operations at this site have not been performed yet | Fracturing operations at this site have not been performed yet |

## 4. EGS Prospects in Poland

In recent years, the interest in obtaining energy from EGS collectors in Poland has increased. The restrictive EU regulations on greenhouse gas emissions and the desire to reduce the share of fossil fuels in the national energy balance encourage the search for new ways of obtaining green energy, including energy from deep geothermal sources. The success of Western European EGS projects sparked a discussion on the profitability of EGS installations in Polish conditions [74,79–81].

Thus far, a preliminary research project was carried out to assess the thermal balance potential of prospective geological structures for the needs of EGS systems in HDR rocks in Poland [2]. The project involved the study of Polish rock structures under three different geological conditions: massifs of crystalline rocks, volcanic rocks under the sedimentary cover and sedimentary basins. The key element of the location selection was the analysis of the Earth's crust temperature on the basis of maps of the Earth's heat flux density distribution in Poland. A series of field geological and geophysical surveys, laboratory tests of rock samples and numerical simulations allow for the determination of several perspective areas [2,82].

Relatively extensive massifs of igneous rocks, useful for EGS technology, are found in the south of Poland (Sudetes and the Fore-Sudetic Block). The most promising area is the granitoid pluton of the Karkonosze Mountains (part of the Sudetes), which is characterized by a geothermal gradient of about 4 °C/100 m, with a temperature of up to 16 °C at a depth of 4.0 km below the ground level (Figure 6). The target zone for stimulation is set up there at a depth of less than 4000 m and a temperature of about 165 °C. $\sigma_V$ in this zone, assuming an average rock density of 2.4 g/cm$^3$ [78], is about 96 MPa in the presumably normal stress regime [75,76].

The Gorzów block is a structure particularly significant in the context of the use of unconventional geothermal resources of volcanic rock. The Permian trachyandesites of the Gorzów Block, located at a depth of below 4300 m, are characterized by large thickness, increased temperatures on a regional scale and contain gas bubbles, which provides good prospects for fracturing. This location shows a significant analogy to the Groß Schönebeck reservoir near Berlin, where the geothermal gradient is 3.5–4.0 °C/100 m, and the temperature reaches approximately 150 °C at a depth of 4.3 km [2,81]. The deposition depth allows to calculate $\sigma_V$ of about 103 MPa.

The largest thicknesses of sedimentary rocks are typical for the central part of the Polish Basin (9–12 km) and the Carpathians (up to approx. 20 km). Due to the complicated geological structure and strong tectonic involvement of the Carpathians [83], this area does not have much potential for the EGS. However, within the Carpathian Foredeep, in the central part of the Upper Silesian Block, an area with increased values of the Earth's heat flux was identified.

The intense heat flux is typical for the Variscan fold belt and in the northern zone of the Lower Silesian internodes, where the heat flow values exceeded 107 mW/m$^2$. The Upper Paleozoic, Devonian and Carboniferous formations lie on the Precambrian and Lower Paleozoic sediments in the form of a continuous cover. The lower part of the Carboniferous profile includes carbonates and clastic, flysch and molasse sediments, forming the Upper Silesian Coal Basin. The thickness of carbonates ranges from 200 to 1500 m, while the thickness of the clastic deposits of Carboniferous, which are a potential petrogeothermal reservoir rock, reaches over 5000 m [84]. At considerable depths, the hydraulic conductivity of Carboniferous sandstones is less than 10–8 m/s [85].

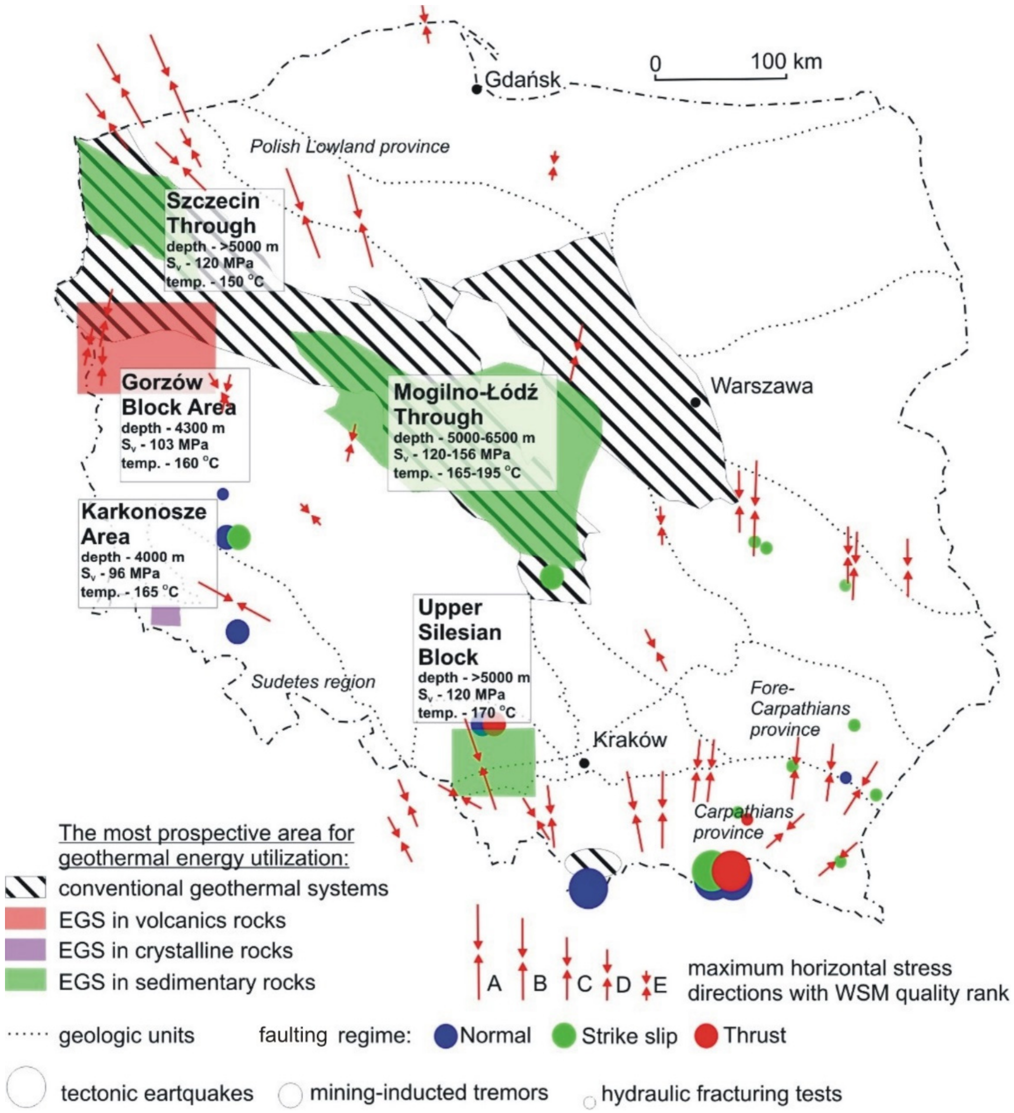


**Figure 6.** Prospective areas for geothermal energy utilization in enhanced geothermal systems in Poland. Explanation: $\sigma_V$ was calculated for given depth, based on average density of overlying rocks—2.4 g/cm$^3$ from [78]. Prospective areas were marked based on data from [74]. Horizontal stress directions and faulting regime were compiled from [75–77,86].

Two areas with potential for EGS were identified in the Polish Lowlands: the Szczecin Trough and the Mogilno-Łódź Trough. The Szczecin Trough is a strongly elongated fold element covering the Zechstein–Mesozoic complex, with a general direction along the NW-SE axis. This form was influenced by the block tectonics of the older basement and the salt tectonics, mobilizing Zechstein salts [87]. Along this structure, a zone of intense halokinetic phenomena occurs. In the area of the Szczecin Trough, which is relatively poorly geologically recognized, the EGS prospects relate to the Permian or Carboniferous sediments at depths above 5000 m below sea level, with temperatures above 150 °C. The deposition depth allows the calculation of vertical principal stress of about 120 MPa. The Mogilno-Łódź Trough is a fragment of a higher-order structure—the Szczecin–Mogilno–Łódź–Miechów Trough, stretching from the northwest to the southeast of Poland.

Potential petrogeothermal reservoirs in this area are Lower Triassic rocks, represented by Buntsandstein sediments deposited at a depth of about 5700 m and developed as a complex of claystone and siltstones with limestone and sandstone beds. The compact sandstones of the Lower Buntsandstein are considered potential deposits for the EGS, especially since their thickness locally exceeds 1500 m. The Middle Triassic (Muschelkalk) formations, formed as limestones and marls, are characterized by a much lower thickness, up to 300 m. The Upper Triassic, with a thickness of up to 2400 m, is represented by clastic and evaporative sediments of Keuper and clayey sandstone deposits of the Rhaetian. The most promising structure for EGS in Poland is the Mogilno–Łódź Trough, while the Upper Silesian Block seems to be a promising location for the future [74].

The legal issues related to the HF implementation in Poland are regulated at European Union and national level. Minimum principles for the exploration and production using HF technology were established in UE Commission recommendations from 22 January 2014 [88]. However, these recommendations concern only hydrocarbons extraction, in terms of high-volume HF (injecting 1000 $m^3$ or more of water per fracturing stage or 10,000 $m^3$ or more of water during the entire fracturing process into a well), whereas fracturing regulations in terms of geothermal resources have not been developed so far. In Poland, there are no internal prohibitions for HF operations; thus, EU Commission recommendations are valid. Assuming that high-volume fracking in HDR would be treated the same as fracking for hydrocarbon extraction, a strategic environmental assessment may be required before granting licenses for exploration or production to prevent, manage and reduce the impacts on and risks for human health and the environment.

Stimulation of HDR horizons and the design of fracturing operations to create a geothermal collector have not been carried out in Poland so far. Nevertheless, the extensive experience was gained in hydraulic and chemical stimulation operations, based on fracturing in unconventional deposits and matrix acidizing [15,89]. Research works were also carried out in the field of the design, environmental impact and performance of energized fluids for fracturing [90]; the embedment phenomena [24,25]; and the dynamic elastic parameters of the various types of rocks [27,30]. Their results may be useful in the implementation of a prospective Polish HDR geothermal collector program.

## 5. Conclusions

In this paper, 10 hydraulically stimulated world's enhanced geothermal systems (EGS) were reviewed. The focus of the review concerned geological, geophysical as well as stimulation parameters.

The target zones in most EGS sites are usually crystalline rocks, i.e., granite or granodiorites, characterized by low permeability and porosity (e.g., Habanero, Pohang, Forge Utah EGS projects). However, in some projects, a geothermal collector is created in mixed, crystalline and low permeable clastic rock, e.g., Groß Schönebeck and GeneSys Hannover EGS projects. These rocks are generally deposited at a depth of 2000–5000 m, whereas the localizations are chosen mostly due to the high geothermal gradient caused by local temperature anomalies near-vertical faults and fractures, connecting the sedimentary cover and crystalline basement, constituting heat-conductive areas. Target zone temperatures are typically between 150 to over 300 °C, which determines the flow rate directly in the heat exchanger and the efficiency of the powerplant. Tectonic field conditions are not the main criterion for selecting an EGS location.

Many of the locations are characterized by normal or strike-slip faulting regimes, while several projects were located in the areas of reverse/overthrust faulting regime (e.g., Habanero, Australia, Fjällbacka, Sweden). The faulting regime directly affects the direction of fracture propagation. It seems that the best conditions for fracturing in EGS are in the reverse regime due to the preferred horizontal fractures capable of connecting vertical boreholes in this area. However, European EGS projects in normal strike-slip faulting regime areas (preferred vertical fracture propagation) were also successful (e.g., Soultz, France, Landau, Germany). The P-wave velocities in crystalline rocks are usually in the range of about 4400–5500 m/s; thus, they are higher than the velocities in typical clastic rocks. Elastic parameters of the crystal base rocks reported in the literature are varied depending on the measurement method. It can be stated that Young's modulus and Poisson's ratio of crystalline rocks from measurements in reservoir conditions are in the range of about 45–75 GPa and 0.12–0.25 (-), respectively.

The range of pressure and pumping rates in hydraulic fracturing (HF) treatments are varied depending on the needs. The amount of water injected into the well is varied from a few thousand up to more than 10,000 $m^3$ (Massive Hydraulic Fracturing operation) during the entire fracturing process. Fresh water without chemical additives in the main fracking stages is commonly used; however, linear as well as crosslinked gels are also applied (i.e., Groß Schönebeck project). In some cases, a 20/40 mesh quartz sand or high-strength proppant is also used. The obtained fracture dimensions depend on the pumping rate, pressure and total pumped liquid volume. The half-length and height of the fracture may reach more than several hundred meters, whereas width may exceed several centimeters, which determines the distance between bottoms of the boreholes.

HF operations usually cause seismic events recorded by installed seismic monitoring. The most common are low-magnitude events, imperceptible to people; however, there are also large ones, i.e., in Pohang, Korea, in 2017. The liquid pumped under pressure during the HF operation may facilitate skidding on the stressed local fault surfaces, which in unfavorable conditions may generate seismic events; however, shocks with a relatively high magnitude are rare.

The success of the Western European EGS projects caused a discussion on the profitability of the EGS-type installation in Polish conditions. The preliminary research project has been carried out so far to assess the thermal balance potential of prospective geological structures for the needs of EGS systems in HDR rocks in Poland. Based on the set of the Earth's heat flux density distribution data in Poland, several main prospective areas were finally selected. The most promising formations are the crystalline basement of Karkonosze Mountains, volcanic rocks of Gorzów Block and sedimentary deposits of the Szczecin Trough, the Mogilno-Łódź Trough and the Upper Silesian Block.

**Author Contributions:** Conceptualization, literature review, investigation, manuscript writing, visualization, R.M.; supervision, literature review, investigation, manuscript editing, manuscript review, K.L.; supervision, manuscript editing, manuscript review, founding acquisition, P.K. All authors have read and agreed to the published version of the manuscript.

**Funding:** This paper is based on the research carried out in the Oil and Gas Institute - National Research Institute (Poland), financed by Ministry of Education and Science of Poland. DK-4100-18/21.

**Institutional Review Board Statement:** Not applicable.

**Informed Consent Statement:** Not applicable.

**Data Availability Statement:** The data presented in this study are available on request from the corresponding author.

**Conflicts of Interest:** The authors declare no conflict of interest.

## Nomenclature

| | |
|---|---|
| HF | Hydraulic fracturing |
| MHF | Massive hydraulic fracturing |
| EGS | Enhanced geothermal systems |
| HDR | Hot dry rock |
| $\sigma_V$ | Principal vertical stress (MPa) |
| $\sigma_H$ | Maximum horizontal stress (MPa) |
| $\sigma_h$ | Minimum horizontal stress (MPa) |
| $P_p$ | Pore pressure (MPa) |
| $V_P$ | Compressional wave velocity (m/s) |
| $V_S$ | Shear wave velocity (m/s) |
| $E$ | Young's modulus (GPa) |
| $v$ | Poisson's ratio (dimensionless) |

## References


1. Lu, S.-M. A global review of enhanced geothermal system (EGS). *Renew. Sustain. Energy Rev.* **2018**, *81*, 2902–2921. [CrossRef]
2. Wójcicki, A.; Sowiżdżał, A.; Bujakowski, W. *Ocena Potencjału Bilansu Cieplnego i Perspektywicznych Struktur Geologicznych dla Potrzeb Zamkniętych Systemów Geotermicznych (Hot Dry Rocks) w Polsce*; Ministerstwo Środowiska: Warsaw, Poland, 2013. (In Polish)
3. Zhang, H.; Wan, Z.; Elsworth, D. Failure behavior of hot-dry-rock (HDR) in enhanced geothermal systems: Macro to micro scale effects. *Geofluids* **2020**, *2020*, 8878179. [CrossRef]
4. McClure, M.; Horne, R. An investigations of stimulation mechanisms in enhanced geothermal systems. *Int. J. Rock Mech. Min. Sci.* **2014**, *72*, 242–260. [CrossRef]
5. Vidal, J.; Genter, A.; Schmittbuhl, J. Pre- and post-stimulation characterization of geothermal well GRT-1, Rittershoffen, France: Insights from acoustic image logs of hard fractured rock. *Geophys. J. Int.* **2007**, *206*, 845–860. [CrossRef]
6. Economides, M.; Martin, T. *Modern Fracturing Enhancing Natural Gas Production*; ET Publishing: Houston, TX, USA, 2007.
7. Brown, D.; Duchane, D.; Heiken, G.; Hriscu, V. *Mining the Earth's Heat: Hot Dry Rock Geothermal Energy*; Springer: Berlin/Heidelberg, Germany, 2012.
8. Hills, R.; Hand, M.; Mildren, S.; Morton, J.; Reid, P.; Reynolds, S. Hot dry rock geothermal exploration in Australia, application of the in situ stress field to hot dry rock geothermal energy in the Cooper Basin. In Proceedings of the PESA Eastern Australian Basins Symposium II, Adelaide, Australia, 19–22 September 2004.
9. Schellschmidt, R.; Schultz, R.; Pester, S. Geothermal energy in Germany. In Proceedings of the World Geothermal Congress, Bali, Indonesia, 25–29 April 2010.
10. Huenges, E. *Geothermal Energy Systems: Exploration, Development and Utilization*; Wiley-VCH: Weinheim, Germany, 2010.
11. King, G. Thirty years of gas shale fracturing: What we have learned? In Proceedings of the SPE Annual Technical Conference and Exhibition, Florence, Italy, 20–22 September 2010. [CrossRef]
12. Gandossi, L. *An Overview of Hydraulic Fracturing and Other Formation Stimulation Technologies for Shale Gas Production*; JRC Technical Reports; Publications Office of the European Union: Luxembourg, 2013. [CrossRef]
13. Yildizdag, K.; Weber, F.; Konietzky, H. Hydraulic Fracturing. Available online: https://tu-freiberg.de/sites/default/files/media/professur-felsmechanik-32204/E-book/15_hydraulic_fracturing_0.pdf (accessed on 2 February 2021).
14. Rafiee, M.; Soliman, M.; Pirayesh, E.; Meybodi, H. Geomechanical considerations in hydraulic fracturing designs. In Proceedings of the SPE Canadian Unconventional Resources Conference, Calgary, AB, Canada, 30 October–1 November 2012. [CrossRef]
15. Kasza, P. Hydraulic fracturing in unconventional reservoirs and methods of their analysis. *Prace INiG-PIB* **2019**, *226*. (In Polish with English Abstract). [CrossRef]
16. Tester, J.; Anderson, B.; Batchelor, A.; Blackwell, D.; DiPippo, R.; Drake, M.; Garnish, J.; Livesay, B.; Moore, M.; Nichols, K.; et al. *The Future of Geothermal Energy—Impact of Enhanced Geothermal Systems (EGS) on the United States in the 21st Century*; Massachusetts Institute of Technology: Cambridge, MA, USA; Idaho National Laboratory: Idaho Falls, ID, USA, 2006.
17. Park, S.; Kim, K.-I.; Xie, L.; Yoo, H.; Min, K.-B.; Kim, M.; Yoon, B.; Kim, K.Y.; Zimmermann, G.; Guinot, F.; et al. Observations and analyses of the first two hydraulic stimulations in the Pohang geothermal development site, South Korea. *Geothermics* **2020**, *88*, 101905. [CrossRef]
18. Legarth, B.; Huenges, E.; Zimmermann, G. Hydraulic fracturing in a sedimentary geothermal reservoir: Results and implications. *Int. J. Rock Mech. Min. Sci.* **2005**, *42*, 1028–1041. [CrossRef]
19. Zoback, M. *Reservoir Geomechanics*; Cambrige University Press: Cambrige, UK, 2007. [CrossRef]
20. Zimmermann, G.; Moeck, I.; Blöcher, G. Cyclic waterfrac stimulation to develop an enhanced geothermal system (EGS): Conceptual design and experimental results. *Geothermics* **2010**, *39*, 59–69. [CrossRef]
21. Zimmermann, G.; Blöcher, G.; Reinicke, A.; Brandt, W. Rock specific hydraulic fracturing and matrix acidizing to enhance a geothermal system—Concepts and field results. *Tectonophysics* **2011**, *503*, 146–154. [CrossRef]
22. Rickman, R.; Mullen, M.; Petre, E.; Grieser, B.; Kundert, D. A Practical use of shale petrophysics for stimulation designing optimalization: All shale plays are not clones of the Barnett Shale. In Proceedings of the SPE Annual Technical Conference and Exhibition, Denver, CO, USA, 21–24 September 2008. [CrossRef]
23. Masłowski, M.; Biały, E. Studies of the embedment phenomenon in stimulation treatments. *Nafta-Gaz* **2016**, *12*, 1101–1106. [CrossRef]
24. Masłowski, M.; Kasza, P.; Czupski, M.; Wilk, K.; Moska, R. Studies of fracture damage caused by the proppant embedment phenomenon in shale rock. *Appl. Sci.* **2019**, *9*, 2190. [CrossRef]
25. Masłowski, M.; Labus, M. Preliminary studies on the proppant embedment in Baltic Basin shale rock. *Rock Mech. Rock Eng.* **2021**, *54*, 2233–2248. [CrossRef]
26. Grieser, W.; Bray, J. Identification of production potential in unconventional reservoirs. In Proceedings of the Production and Operations Symposium, Oklahoma City, OK, USA, 1–3 April 2007. [CrossRef]
27. Moska, R.; Kasza, P.; Masłowski, M. Rock anisotropy and brittleness from laboratory ultrasonic measurements in the service of hydraulic fracturing. *Acta Geodyn. Geomater.* **2018**, *15*, 1. [CrossRef]
28. Moska, R.; Masłowski, M. Attempts to determine the geomechanical and Thomsen's anisotropy parameters of coal from Upper Silesian Coal Basin area. *Nafta-Gaz* **2019**, *11*, 700–707. [CrossRef]
29. Wu, H.; Zhang, P.; Dong, S.; Huang, Y.; Zhang, M. Brittleness index analysis of coal samples. *Acta Geophys.* **2019**, *67*, 789–797. [CrossRef]

30. Moska, R. Brittleness index of coal from the Upper Silesian Coal Basin. *Acta Geodyn. Geomater.* **2021**, *18*, 91–101. [CrossRef]
31. Duffield, R.; Nunz, G.; Smith, M.; Wilson, M. *Hot Dry Rock Geothermal Energy Development Program Annual Report, Fiscal Year 1980*; Los Alamos National Lab: Santa Fe, NM, USA, 1980.
32. Norbeck, J.; McClure, M.; Horne, R. Field observations at the Fenton Hill enhanced geothermal system test site support mixed-mechanism stimulation. *Geothermics* **2018**, *74*, 135–149. [CrossRef]
33. Wyborn, D.; da Graaf, L.; Davidson, S.; Hann, S. Development of Australia's first hot fractured rock (HFR) underground heat exchanger, Cooper Basin, South Australia. In Proceedings of the World Geothermal Congress, Antalya, Turkey, 24–29 April 2005.
34. Holl, H.-G. *What Did We Learn about EGS in the Cooper Basin?* Geodynamics Limited Technical Report; Geodynamics Limited: Milton, Australia, 2015. [CrossRef]
35. Holl, H.-G.; Barton, C. Habanero Field—Structure and state of stress. In Proceedings of the World Geothermal Congress, Melbourne, Australia, 19–25 April 2015.
36. Barton, C.; Moos, D.; Hartley, L.; Baxter, S.; Foulquier, L.; Holl, H.; Hogarth, R. Geomechanically coupled simulation of flow in fractured reservoirs. In Proceedings of the 38th Workshop on Geothermal Reservoir Engineering, Stanford, CA, USA, 11–13 February 2013.
37. Hogarth, R.; Holl, H.-G. Lessons learned from the habanero EGS project. In Proceedings of the Transactions—Geothermal Resources Council, Salt Lake City, UT, USA, 2–4 October 2017.
38. Australian Broadcast Corporation News. Available online: https://www.abc.net.au/news/2016-08-30/geothermal-power-plant-closes-deemed-not-financially-viable/7798962 (accessed on 4 May 2021).
39. Vidal, J.; Genter, A. Overview of naturally permeable fractured reservoirs in the central and southern Upper Rhine Graben: Insights from geothermal wells. *Geothermics* **2018**, *74*, 57–73. [CrossRef]
40. Cuenot, N.; Charlety, J.; Dorbath, L.; Hasser, H. Faulting mechanisms and stress tensor at the European HDR site of Soultz-Sous-Forêts. In Proceedings of the Thirtieth Workshop on Geothermal Reservoir Engineering, Stanford, CA, USA, 31 January–2 February 2005.
41. Schindler, M.; Nami, P.; Schellschmidt, R.; Teza, D.; Tischner, T. Summary of hydraulic stimulation operations in the 5 km deep crystalline HDR/EGS reservoir at Soults-sous-Forets. In Proceedings of the 33th Workshop on Geothermal Reservoir Engineering, Stanford, CA, USA, 28–30 January 2008.
42. Schindler, M.; Baumgärtner, J.; Gandy, T.; Hauffe, P.; Hettkamp, T.; Menzel, H.; Penzkofer, P.; Teza, D.; Tischner, T.; Wahl, G. Successful hydraulic stimulation techniques for electric power production in the Upper Rhine Graben, Central Europe. In Proceedings of the World Geothermal Congress, Bali, Indonesia, 25–29 April 2010.
43. BESTEC GmbH. Available online: https://www.bestec-for-nature.com/index.php/projects-en (accessed on 19 March 2021).
44. Baujard, C.; Genter, A.; Dalmais, E.; Maurer, V.; Hehn, R.; Rosillette, R.; Vidal, J.; Schmittbuhl, J. Hydrothermal characterization of wells GRT-1 and GRT-2 in Rittershoffen, France: Implications on the understanding of natural flow systems in the Rhine graben. *Geothermics* **2017**, *65*, 255–268. [CrossRef]
45. Baujard, C.; Genter, A.; Maurer, V.; Dalmais, E.; Graff, J.-J.; Schmittbuhl, J. The ECOGI EGS Project in Rittershoffen, France. *GRC Transactions* **2014**, *38*, 267–270.
46. Maurer, V.; Baujard, C.; Gaucher, E.; Grunberg, M.; Wodling, H.; Lehujeur, M.; Vergne, J.; Lengline, O.; Schmittbuhl, J. Seismic monitoring of the Rittershoffen project (Alsace, France). In Proceedings of the 2nd European Geothermal Workshop, Strasbourg, France, 24–25 October 2013.
47. Lengline, O.; Boubacar, M.; Schmittbuhl, J. Seismicity related to the hydraulic stimulation of GRT1, Rittershoffen, France. *Geophys. J. Int.* **2017**, *208*, 1704–1715. [CrossRef]
48. ES Geotermie. Available online: https://geothermie.es.fr/en/ (accessed on 13 July 2021).
49. Ladner, F.; Häring, M. Hydraulic characteristics of the Basel-1 enhanced geothermal system. *GRC Trans.* **2009**, *33*, 199–204.
50. Orzol, J.; Jung, R.; Jatho, R.; Tischner, T.; Kehrer, P. The GeneSys-Project: Extraction of geothermal heat from tight sediments. In Proceedings of the World Geothermal Congress, Antalya, Turkey, 24–29 April 2005.
51. Tischner, T.; Evers, H.; Hauswirth, H.; Jatho, R.; Kosinowski, M.; Sulzbacher, H. New concepts for extracting geothermal energy from one well: The GeneSys project. In Proceedings of the World Geothermal Congress, Bali, Indonesia, 25–29 April 2010.
52. Tischner, T.; Krug, S.; Pechan, E.; Hesshaus, A.; Jatho, R.; Bischoff, M.; Wonik, T. Massive hydraulic fracturing in low permable sedimentary rock in the Genesys project. In Proceedings of the 38th Workshop on Geothermal Reservoir Engineering, Stanford, CA, USA, 11–13 February 2013.
53. Holl, H.-G.; Moeck, I.; Schandelmeier, H. Characterisation of the tectono-sedimentary evolution of a geothermal reservoir—Implications for exploitation (southern permian basin, NE Germany). In Proceedings of the Word Geothermal Congress 2005, Antalya, Turkey, 24–29 April 2005.
54. Huenges, E.; Holl, H.-G.; Bruhn, D.; Brandt, W.; Saadat, A.; Moeck, I.; Zimmermann, G. Current state of the EGS project Groß Schönebeck—Drilling into the deep sedimentary geothermal reservoir. In Proceedings of the European Geothermal Congress 2007, Unterhaching, Germany, 30 May–1 June 2007.
55. Blöcher, G.; Reinsch, T.; Henninges, J.; Milsch, H.; Regensprug, S.; Kummerow, J.; Francke, H.; Kranz, S.; Saadat, A.; Zimmermann, G.; et al. Hydraulic history and current state of the deep geothermal reservoir Groß Schönebeck. *Geothermics* **2015**, *63*, 27–43. [CrossRef]

56. Hassanzadegan, A.; Blöcher, G.; Zimmermann, G.; Milsch, H.; Moeck, I. Induced stress in a geothermal doublet system. In Proceedings of the Thirty-Sixth Workshop on Geothermal Reservoir Engineering, Stanford, CA, USA, 31 January–2 February 2011.
57. Moeck, I.; Holl, H.-G. The stress regime in Rotliegend reservoir of the Northeast German Basin. *Int. J. Earth Sci.* **2009**, *98*, 1643–1657. [CrossRef]
58. Farkas, M.P.; Hofman, H.; Zimmermann, G.; Zang, A.; Bethmann, F.; Cottrell, M.; Josephson, N. Hydromechanical analysis of the second hydraulic stimulation in well PX-1. *Geothermics* **2021**, *89*, 101990. [CrossRef]
59. Lee, T.J.; Song, Y. Lesson learned from low-temperature geothermal development in Pohang, Korea. In Proceedings of the 8th Asian Geothermal Symposium, Hanoi, Vietnam, 9–10 December 2008.
60. Kwon, S.; Xie, L.; Park, S.; Kim, K.-I.; Min, K.-B.; Kim, K.Y.; Zhuang, L.; Choi, J.; Kim, H.; Lee, T.J. Characterization of 4.2-km-deep fractured granodiorite cores from Pohang geothermal reservoir, Korea. *Rock Mech. Rock Eng.* **2019**, *52*, 771–782. [CrossRef]
61. Hofmann, H.; Zimmermann, G.; Farkas, M.; Huegenes, E.; Zang, A.; Leonhardt, M.; Kwiatek, G.; Martinez-Garzon, P.; Bonhoff, M.; Min, K.-B.; et al. First field application of cyclic soft stimulation at the Pohang Enhanced Geothermal System site in Korea. *Geophys. J. Int.* **2019**, *217*, 926–949. [CrossRef]
62. Ellsworth, W.L.; Giardini, D.; Townend, J.; Ge, S.; Shimamoto, T. Triggering of the Pohang, Korea, earthquake (Mw 5.5) by enhanced geothermal system stimulation. *Seismol. Res. Lett.* **2019**, *90*, 1844–1858. [CrossRef]
63. Ree, J.-H.; Kim, K.-H.; Lim, H.; Seo, W.; Kim, S.; An, X.; Kim, Y. Fault reactivation and propagation during the 2017 Pohang earthquake sequence. *Geothermics* **2021**, *92*, 102048. [CrossRef]
64. Jones, C.; Moore, J.; Simmons, S. Lithology and Mineralogy of the Utah FORGE EGS Reservoir: Beaver County, Utah. *GRC Trans.* **2018**, *42*. Available online: https://publications.mygeoenergynow.org/grc/1034039.pdf (accessed on 1 September 2021).
65. Moore, J.; McLennan, J.; Pankow, K.; Simmons, S.; Podgorney, R.; Wannamaker, P.; Jones, C.; Rickard, W.; Xing, P. The Utah Frontier Observatory for Research in Geothermal Energy (FORGE): A Laboratory for characterizing, creating and sustaining enhanced geothermal systems. In Proceedings of the 45th Workshop on Geothermal Reservoir Engineering, Stanford, CA, USA, 10–12 February 2020.
66. Xing, P.; McLennan, J.; Moore, J. In-situ stress measurements at the Utah Frontier Observatory for Research in Geothermal Energy (FORGE) site. *Energies* **2020**, *13*, 5842. [CrossRef]
67. US Departament of Energy. Available online: https://www.energy.gov/eere/forge/enhanced-geothermal-systems (accessed on 23 March 2021).
68. Lei, Z.; Zhang, Y.; Yu, Z.; Hu, Z.; Li, L.; Zhang, S.; Fu, L.; Zhou, L.; Xie, Y. Exploratory research into the enhanced geothermal system power generation project: The Qiabuqia geothermal field, Northwest China. *Renew. Energy* **2019**, *139*, 52–70. [CrossRef]
69. Lei, Z.; Zhang, Y.; Zhang, S.; Fu, L.; Hu, Z.; Yu, Z.; Li, L.; Zhou, J. Electricity generation from a three-horizontal-well enhanced geothermal system in the Qiabuqia geothermal field, China: Slickwater fracturing treatments for different reservoir scenarios. *Renew. Energy* **2020**, *145*, 65–83. [CrossRef]
70. Meller, C.; Ledesert, B. Is there a link between mineralogy, petrophysics, and the hydraulic and seismic behaviors of the Soultz-sous-Forêts granite during stimulation? A review and reinterpretation of petro-hydromechanical data toward a better understanding of induced seismicity and fluid flow. *J. Geophys. Res. Solid Earth* **2017**, *112*, 9755–9774. [CrossRef]
71. Park, S.; Xie, L.; Kim, K.-I.; Kwon, S.; Min, K.-B.; Choi, J.; Yoon, W.-S.; Song, Y. First hydraulic stimulation in fractured geothermal reservoir in Pohang PX-2 well. *Procedia Eng.* **2017**, *191*, 829–837. [CrossRef]
72. US Departament of Energy. Enhanced Geothermal System Testing and Development at the Milford, Utah FORGE Site. 2016. Available online: https://www.energy.gov/sites/prod/files/2016/09/f33/Conceptual_Geologic_Model_FORGE_Milford_UT.pdf (accessed on 23 March 2021).
73. Feng, J.; Zhang, Y.; Luo, J. Geology of hot dry rocks in Gonghe Basin of Qinghai-Tibet Plateau. In Proceedings of the 54th U.S. Rock Mechanics/Geomechanics Symposium, Golden, CO, USA, 28 June–1 July 2020. ARMA-2020-0011.
74. Sowiżdżał, A.; Gładysz, P.; Pająk, L. Sustainable use of petrothermal resources—A review of the geological conditions in Poland. *Resources* **2021**, *10*, 8. [CrossRef]
75. Jarosiński, M. Recent tectonic stress field investigations in Poland: A state of the art. *Geol. Quaterly* **2005**, *50*, 303–321.
76. Zuchiewicz, W.; Badura, J.; Jarosiński, M. Neotectonics of Poland: Selected examples. *Biul. Państwowego Inst. Geol.* **2007**, *425*, 105–128, (In Polish with English Abstract).
77. Jarosiński, M. Rozwarstwienie współczesnego pola naprężeń w zachodniej części polskich Karpat Zewnętrznych. *Przegląd Geol.* **1997**, *45*, 768–776. (In Polish)
78. Jarosiński, M. Współczesny reżim tektoniczny w Polsce na podstawie analizy testów szczelinowania hydraulicznego ścian otworów wiertniczych. *Przegląd Geol.* **2005**, *53*, 863–872. (In Polish)
79. Sapińska-Śliwa, A.; Kowalski, T.; Knez, D.; Śliwa, T.; Gonet, A.; Bieda, A. Geological and drilling aspects of construction and exploitation geothermal systems HDR/EGS. *AHG Drill. Oil Gas* **2015**, *31*, 49–62. [CrossRef]
80. Niezgoda, T.; Miedzińska, D.; Sławiński, G. Energia z głębokich pokładów gorących suchych skał (HDR). *Inżynieria Bezpieczeństwa Obiektów Antropog.* **2018**, *3–4*, 65–69. (In Polish)
81. Sowiżdżał, A. Geothermal energy resources in Poland—Overview of the current state of knowledge. *Renew. Sustain. Energy Rev.* **2018**, *82*, 4020–4027. [CrossRef]

82. Sowiżdżał, A.; Górecki, W.; Hajto, M. Geological conditions of geothermal resource occurrences in Poland. *Geol. Q.* **2020**, *64*, 185–196. [CrossRef]
83. Górecki, W. (Ed.) *Atlas of Geothermal Waters and Energy Resources in the Western Carpathians*; Ministry of Environment of Poland, ZSE AGH: Krakow, Poland, 2011.
84. Buła, Z.; Żaba, J. Pozycja tektoniczna Górnośląskiego Zagłębia Węglowego na tle prekambryjskiego i dolnopaleozoicznego podłoża. In *Geologia i Zagadnienia Ochrony Środowiska w Regionie Górnośląskim*; Jureczka, J., Buła, Z., Żaba, J., Eds.; Polish Geological Institute, Polish Geological Society: Warsaw, Poland, 2005. (In Polish)
85. Różkowski, A. (Ed.) *Środowisko Hydrogeochemiczne Karbonu Produktywnego Górnośląskiego Zagłębia Węglowego*; Prace Naukowe Uniwersytetu Śląskiego w Katowicach; University of Silesia: Katowice, Poland, 2004. (In Polish)
86. Heidbach, O.; Rajabi, M.; Cui, X.; Fuchs, K.; Muller, B.; Reinecker, J.; Reiter, K.; Tingay, M.; Wenzel, F.; Xie, F.; et al. The world stress map database release 2016: Crustal stress pattern across scales. *Tectonophysics* **2018**, *744*, 484–498. [CrossRef]
87. Miecznik, M.; Sowiżdżał, A.; Tomaszewska, B.; Pająk, L. Modelling geothermal conditions in part of the Szczecin Trough—The Chociwel Area. *Geologos* **2015**, *21*, 187–196. [CrossRef]
88. *European Union Commission Recommendation of 22 January 2014 on Minimum Principles for the Exploration and Production of Hydrocarbons (Such as Shale Gas) Using High-Volume Hydraulic Fracturing (2014/70/EU)*; European Union Commission: Brussels, Belgium, 2014.
89. Czupski, M.; Kasza, P.; Leśniak, Ł. Development of selective acidizing technology for an oil field in the Zechstein main dolomite. *Energies* **2020**, *13*, 5940. [CrossRef]
90. Wilk, K.; Kasza, P.; Labus, K. Impact of Nitrogen Foamed Stimulation Fluids Stabilized by Nanoadditives on Reservoir Rocks of Hydrocarbon Deposits. *Nanomaterials* **2019**, *9*, 766. [CrossRef]